MOLECULAR AND CELLULAR BIOLOGY, Jan. 2008, p. 177–187 Vol. 28, No. 1
0270-7306/08/$08.00+0 doi:10.1128/MCB.00880-07

The Xeroderma Pigmentosum Group E Gene Product DDB2 Activates Nucleotide Excision Repair by Regulating the Level of $p21^{Waf1/Cip1}$▽†

Tanya Stoyanova, Taewon Yoon,‡ Dragana Kopanja, Margalit B. Mokyr, and Pradip Raychaudhuri*

Department of Biochemistry and Molecular Genetics (M/C 669), University of Illinois at Chicago, 900 South Ashland Avenue, Chicago, Illinois 60607

Received 18 May 2007/Returned for modification 12 June 2007/Accepted 21 October 2007

The xeroderma pigmentosum group E gene product DDB2, a protein involved in nucleotide excision repair (NER), associates with the E3 ubiquitin ligase complex Cul4A-DDB1. But the precise role of these interactions in the NER activity of DDB2 is unclear. Several models, including DDB2-mediated ubiquitination of histones in UV-irradiated cells, have been proposed. But those models lack clear genetic evidence. Here we show that DDB2 participates in NER by regulating the cellular levels of $p21^{Waf1/Cip1}$. We show that DDB2 enhances nuclear accumulation of DDB1, which binds to a modified form of p53 containing phosphorylation at Ser18 ($p53^{S18P}$) and targets it for degradation in low-dose-UV-irradiated cells. $DDB2^{-/-}$ mouse embryonic fibroblasts (MEFs), unlike wild-type MEFs, are deficient in the proteolysis of $p53^{S18P}$. Accumulation of $p53^{S18P}$ in $DDB2^{-/-}$ MEFs causes higher expression $p21^{Waf1/Cip1}$. We show that the increased expression of $p21^{Waf1/Cip1}$ is the cause NER deficiency in $DDB2^{-/-}$ cells because deletion or knockdown of $p21^{Waf1/Cip1}$ reverses their NER-deficient phenotype. $p21^{Waf1/Cip1}$ was shown to bind PCNA, which is required for both DNA replication and NER. Moreover, an increased level of $p21^{Waf1/Cip1}$ was shown to inhibit NER both in vitro and in vivo. Our results provide genetic evidence linking the regulation of $p21^{Waf1/Cip1}$ to the NER activity of DDB2.

The UV rays in sunlight are considered to be the major cause of skin cancers. UV causes DNA damage by generating cyclobutane pyrimidine dimers (CPDs) and 6-4 photoproducts, which are repaired mainly by the nucleotide excision repair (NER) pathway (reviewed in reference 41). NER involves excision of the strand containing CPDs or 6-4 photoproducts, followed by repair synthesis to fill the gap. Several genes involved in NER are mutated in xeroderma pigmentosum, a rare repair deficiency disease in which the patients are sun sensitive and develop skin cancer at a high frequency (see references 11 and 16 for reviews). Eight complementation groups, XPA through XPG and XPV, have been characterized in xeroderma pigmentosum. While XPV encodes an error-prone DNA polymerase, the other XP genes encode proteins that participate in the excision of the damaged DNA strand. For example, XPC participates in the recognition of damaged DNA. Subsequently, XPB and XPD participate in unwinding the strands at the damaged site; XPA is critical for positioning the endonucleases XPF and XPG with respect to the damaged site, leading to excision of the damaged strand. The gap generated following excision is filled by DNA polymerase delta that involves PCNA to carry out the repair synthesis (41). Thus, while all other XP genes have been functionally characterized, the mechanism by which the XPE gene participates in NER has remained controversial.

The XPE gene encodes DDB2, a subunit of the damaged-DNA-binding protein DDB, which possesses a high affinity for CPDs and 6-4 photoproducts (reviewed in reference 48). Cells from XP-E patients exhibit a deficiency in NER. The NER deficiency in XP-E cells, along with several other in vivo studies, suggested a role for DDB2 in NER (25, 36, 48). Studies with $DDB2^{-/-}$ mice provided further evidence of a role for DDB2 in inhibiting UV-induced skin carcinogenesis (3, 22, 54), a characteristic of the XP gene products.

Because of the high affinity of DDB, a complex of DDB1 and DDB2, for damaged DNA, several studies have implicated DDB2 and DDB in the early damaged-DNA recognition step of NER. However, a direct role for DDB2 or DDB in NER is a point of controversy. Initial studies reported a stimulatory activity of DDB in NER assays in vitro (51). However, two recent studies carried out thorough analyses of the NER activities of DDB (26, 40). Those studies failed to detect any significant NER activity of DDB2 and its associated proteins. It is noteworthy that the in vitro studies were carried out with naked DNA and the assays analyzed the efficiency of excision of the damaged strand. Those studies did not rule out a role for DDB2 in repair in the context of chromatin or a role for DDB2 downstream of excision. Interestingly, DDB2 was shown also to associate with the CBP/p300 family of histone acetyltransferases and it was suggested that DDB participates in NER through remodeling of chromatin at damaged sites (13, 39).

We showed that DDB2, along with DDB1, associates with Cul4A (46). Moreover, Cul4A induces proteolysis of DDB2 through the ubiquitin-proteasome pathway and this proteolysis plays a significant role in regulating the level of DDB2 in S phase of the cell cycle (34). Interestingly, DDB2 also associates

* Corresponding author. Mailing address: Department of Biochemistry and Molecular Genetics (M/C 669), University of Illinois at Chicago, 900 South Ashland Avenue, Chicago, IL 60607. Phone: (312) 413-0255. Fax: (312) 355-3847. E-mail: Pradip@uic.edu.

† Supplemental material for this article may be found at http://mcb.asm.org/.

‡ Present address: Ben May Institute for Cancer Research, University of Chicago, Chicago, IL 60637.

▽ Published ahead of print on 29 October 2007.

with the COP9 signalosome, which is believed to participate in this proteolysis through the ubiquitin-proteasome pathway (17). Degradation of DDB2 was observed also in UV-irradiated cells; it was shown that DDB2 is degraded within hours following UV irradiation (3, 14). However, the Cul4A-mediated proteolysis of DDB2 did not explain why a stable complex containing Cul4A, DDB1, and DDB2 could be detected in cell extracts (46). Recent studies have provided some insight regarding a functional role of the stable association of DDB2 with the Cul4A-DDB1 ligase. It has been suggested that the Cul4A-DDB1-DDB2 complex could participate in NER through ubiquitination of histones. For example, one study indicated that DDB2 functions as an adaptor for ubiquitination of histone H2A by the Cul4A-DDB1 ligase and suggested a role for H2A ubiquitination in the NER function of DDB2 (24). The other study identified Cul4-DDB1-DDB2 as the ubiquitin ligase of histones H3 and H4 and suggested that the ubiquitination of H3/H4 is important for recruiting the NER factor XPC to UV-damaged chromatin (52). Those studies also implied a role for Cul4A and Cul4B in the NER process. While those studies provided evidence of a role for Cul4-DDB1-DDB2 in ubiquitinating histones, the role of histone ubiquitination in NER has yet to be established.

A role for Cul4A-DDB1-DDB2 in the recruitment of XPC was suggested also by other studies. For example, one group suggested that the proteolysis of DDB2 by Cul4A is important for the recruitment of XPC to UV-damaged DNA (14). Those authors showed that depletion of Cul4A by small interfering RNA (siRNA) inhibited the recruitment of XPC onto damaged chromatin. Those studies linked the proteolysis of DDB2 to enhanced recruitment of XPC. However, the idea of enhanced XPC recruitment by DDB2 proteolysis is apparently at odds with studies by other groups. For example, Chen et al. (10) studied the role of c-Abl in regulating the function of DDB2. They showed that c-Abl enhanced the polyubiquitination and proteolysis of DDB2 by activating Cul4A. Moreover, those authors correlated the enhanced proteolysis of DDB2 to inhibition of NER by the c-Abl proto-oncoprotein. The apparently opposite observation could be a result of a different context, i.e., proteolysis of DDB2 at the site of damage versus damaged-site-independent proteolysis of DDB2. In another study, Zotter et al. (57) investigated the rate of XPG recruitment at the damaged chromatin. XPG is recruited by XPA, which in turn depends upon the recognition of damaged chromatin by XPC. Surprisingly, those authors did not see any difference in the rate of XPG recruitment between DDB2-proficient and DDB2-deficient cells. Their results argue against a role for DDB2 in the assembly of the excision complex.

DDB2 possesses a nuclear import function (34, 45), and it is important for the nuclear accumulation of the DDB1 subunit of DDB. The naturally occurring mutant forms of DDB2, identified from XP-E patients, are deficient in enhancing the nuclear accumulation of DDB1 (45). However, the significance of the DDB2-mediated nuclear accumulation of DDB1 has not been studied in detail. In this study, using DDB2$^{-/-}$ mouse embryonic fibroblasts (MEFs), we describe a new function of DDB1/DDB2 in the proteolysis of p53 that is phosphorylated at residue Ser18 (p53^{S18P}). Previous studies showed that Cul4A-DDB1 cooperated with MDM2 in the proteolysis of p53 (5, 35). Here we show that the DDB2-mediated nuclear accumulation of DDB1 is important for the proteolysis of p53^{S18P} following low-dose UV irradiation. In DDB2$^{-/-}$ cells, the proteolysis of p53^{S18P} is inefficient and they accumulate p53^{S18P}, leading to higher expression of p21$^{Waf1/Cip1}$. Interestingly, deletion of p21$^{Waf1/Cip1}$ eliminates the repair deficiency in DDB2$^{-/-}$ MEFs. These results provide genetic evidence of a link between the regulation of p21$^{Waf1/Cip1}$ and the NER function of DDB2.

MATERIALS AND METHODS

Mice and MEFs. p21$^{Waf1/Cip1-/-}$ mice were kindly provided by A Tyner. DDB2$^{-/-}$ mice were generated in our laboratory as previously described (54). p21$^{-/-}$ mice were crossed with DDB2$^{-/-}$ mice to produce DDB$^{+/-}$ p21$^{+/-}$ progeny. DDB2$^{+/-}$ p21$^{+/+}$ mice were crossed with DDB2$^{+/-}$ p21$^{+/+}$ mice to obtain DDB2$^{-/-}$ and wild-type MEFs and DDB2$^{+/-}$ p21$^{-/-}$ mice. DDB2$^{+/-}$ p21$^{-/-}$ mice were crossed with DDB2$^{+/-}$ p21$^{-/-}$ to obtain p21$^{-/-}$ and DDB2$^{-/-}$ p21$^{-/-}$ MEFs. MEFs were generated from 13.5-day-old embryos and were grown in Dulbecco modified Eagle medium containing 10% fetal bovine serum.

Irradiation. UV irradiation (12 J/m^2) of cells was carried out with a Stratalinker adjusted to UV-C irradiation. Medium was removed, and cells were washed with phosphate-buffered saline (PBS) before irradiation. Following irradiation, cells were supplemented with culture medium. Ionizing radiation (IR) of the MEFs was carried out with a Cs-137 irradiator.

Decay rate and Western blot analysis. For analysis of the decay rates of phospho-p53, the MEFs were treated with cycloheximide (50 μg/ml) for 10 to 60 min. Cells were harvested after washing with PBS. Cells were lysed by suspension in 2 volumes of buffer containing 0.4 M NaCl, 20 mM Tris-HCl (pH 7.5), 0.1% NP-40, 5% (vol/vol) glycerol, 1 mM NaF, 1 mM Na-orthovanadate, and a protease inhibitor cocktail. Extracts (50 to 100 μg) were subjected to sodium dodecyl sulfate–10% polyacrylamide gel electrophoresis, followed by blotting to nitrocellulose. The blots were probed with antibodies to p53^{S15P} (Calbiochem), p53-ab (Santa Cruz), Cdk2 (Santa Cruz), or tubulin (Santa Cruz).

Immunostaining. Cells were grown on glass coverslips and infected with recombinant adenovirus expressing T7 epitope-tagged DDB1 or DDB2 at 50 PFU/cell. One hour after UV irradiation, the cells were fixed in 4% paraformaldehyde in PBS for 20 min at room temperature and washed once with 0.1 M glycine in PBS, followed by permeabilization for 5 min with 0.1% Triton X in PBS. After fixation, the cells were washed four times with PBS (for 5 min each time) and blocked with 5% goat serum for 1 h at room temperature. Cells were incubated with the T7 monoclonal antibody (1:200) for 2 h at room temperature. The cells were then washed five times with PBS (for 5 min each time) and incubated with a 1:500 dilution of fluorescein isothiocyanate-conjugated goat anti-mouse antibody for 40 min at room temperature, followed by 10 washes with PBS (2 min each). The cell nuclei were labeled with 4′,6′-diamidino-2-phenylindole (DAPI; 2 μg/ml) in PBS for 3 min at room temperature. After a final wash in PBS, the cells were mounted on slides with Vectashield (Vector) mounting medium and viewed with a Nikon microscope.

UDS assays. Unscheduled DNA synthesis (UDS) assays with MEFs were performed as previously described (47). Briefly, MEFs were treated with [^{3}H]thymidine for 1 h to identify and distinguish the S-phase cells. Following that, the cells were subjected to UV irradiation (12 J/m^2) and maintained in medium containing [^{3}H]thymidine for 3 h in the absence of serum. The cells were incubated in medium containing unlabeled thymidine for an additional 30 min and then fixed, treated with EM-1 (Amersham), and developed for UDS measurement.

Quantitative reverse transcription-PCR assays. MEFs (wild type or DDB2$^{-/-}$) and HeLa cells (control or expressing DDB2 short hairpin RNA [shRNA]) were either left untreated or UV irradiated (12 J/m^2). Total RNAs were extracted from the treated and untreated cells with Trizol. One microgram of the total RNA was then subjected to DNase I treatment with RQ1 RNase-free DNase I (Invitrogen). The DNase I-treated RNA was then reverse transcribed with an iScript cDNA synthesis kit (Bio-Rad) according to the manufacturer's protocol. PCR amplification was performed in triplicate with the following primers: mouse *p21*, 5′-TTCCGCACAGGAGCAAAGTG-3′ and 5′-AAGTCAAAGTTCCACC GTTCTCG-3′ (annealing temperature, 64°C); mouse *GAPDH* gene, 5′-AACT TTGGCATTGTGGAAGG-3′ and 5′-CCATCCACAGTCTTCTGGGT-3′ (annealing temperature, 60°C); human *p21*, 5′-AGGGGACAGCAGAGGAAG A-3′ and 5′-GGCGTTTGGAGTGGTAGAA-3′ (annealing temperature, 61.2°C); human cyclophilin, 5′-GCAGACAAGGTCCCAAAGACAG-3′ and 5′CACCCTGACACATAAACCCTGG-3′ (annealing temperature, 55.7°C).

Each PCR mixture contained 0.05 μg of cDNA, a 100 nM concentration of each primer, and 1× iQ SYBR green Supermix (Bio-Rad) in a 25-μl volume. Real-time PCR was performed with the MyiQ single-color real-time PCR detection system (Bio-Rad). Melting curve analysis was performed for every reaction, and a single sharp peak was observed. To create a standard curve for relative quantification, the sample that was not treated with UV was chosen as a standard control, diluted in water (1×, 0.2×, and 0.04×), and subjected to real-time quantitative PCR in triplicate. The dilution value (starting quantity) of the standard was plotted against the threshold cycle number at which fluorescence first increased above the background by the use of MyiQ software (Bio-Rad). The expression of the indicated gene in each sample was evaluated with this standard curve. The levels of *p21* mRNA were normalized against the levels of *GAPDH* mRNA (for MEFs) and cyclophilin mRNA (for HeLa cell lines), which were used as internal controls. The change in the levels of *p21* mRNA was calculated by dividing the normalized values of *p21* RNA in the UV-irradiated samples by the normalized values of *p21* mRNA in the nonirradiated samples.

Ubiquitination of p53^{S18P} and p53. p53 ubiquitination was analyzed by a previously described procedure (53).

RESULTS

DDB2$^{-/-}$ MEFs are deficient in UDS. Construction and characterization of DDB2$^{-/-}$ mice have been described previously (54). We showed that DDB2$^{-/-}$ mice are highly susceptible to UV irradiation-induced skin cancer and that the mice developed spontaneous tumors between the ages of 18 and 23 months with 100% penetrance (54). UV irradiation damages DNA by generating CPDs and 6-4 photoproducts. DDB2 was shown to participate in the removal of this damage through the NER pathway (48 and references therein). Surprisingly, we were not able to see a significant difference in the rate of CPD removal in DDB2$^{-/-}$ MEFs compared to that in wild-type MEFs from littermates (data not shown). Therefore, we sought to use a more quantitative assay to compare the NER efficiency in DDB2$^{-/-}$ MEFs with that in wild-type MEFs. We measured UDS, which assays for repair synthesis, in MEFs after UV irradiation by using a previously described procedure (47). UDS measures DNA synthesis induced by UV irradiation in non-S-phase cells. The MEFs were treated with [^{3}H]thymidine for 1 h to identify and distinguish the S-phase cells. Nuclei of the S-phase cells undergo dense labeling (black arrows in Fig. 1, right panel). Following that, the cells were subjected to UV irradiation (12 J/m^2) and maintained in medium containing [^{3}H]thymidine for 3 h in the absence of serum. The cells were incubated in medium containing unlabeled thymidine for an additional 30 min and then fixed, treated with EM-1 (Amersham), and developed for UDS measurement. Levels of UDS were measured by counting grains per non-S-phase cell nucleus (gray arrows in Fig. 1, right panel). A larger fraction of the nuclei from the wild-type MEFs exhibited higher numbers of grains compared to the nuclei from DDB2$^{-/-}$ MEFs (Fig. 1). Thus, as expected from the deficiency found in XP-E cells, DDB2$^{-/-}$ MEFs were deficient in UDS compared to wild-type MEFs.

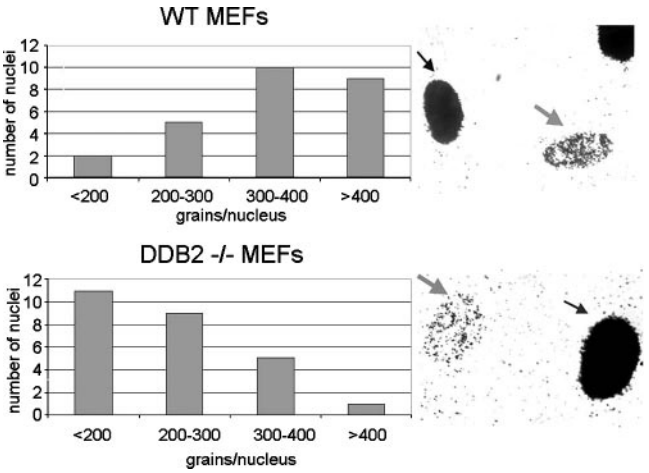

FIG. 1. DDB2$^{-/-}$ MEFs are deficient in NER as measured by UDS. UDS was measured in wild-type (WT) and DDB2$^{-/-}$ MEFs after UV irradiation as previously described (47). The slides were developed for a week. After development, the numbers of grains per nucleus were obtained by counting 25 non-S-phase nuclei per sample. Numbers of grains per nucleus are plotted in the left panels, and autoradiographs of the grains in nuclei are shown in the right panels.

DDB2$^{-/-}$ MEFs are deficient in UV-induced nuclear entry of DDB1. We showed that naturally occurring DDB2 mutants isolated from XP-E patients are deficient in promoting nuclear accumulation of DDB1 (45). Therefore, we investigated whether or not DDB2$^{-/-}$ MEFs are deficient in the nuclear accumulation of DDB1. Specifically, we studied the localization of DDB1 with and without UV or IR. UV irradiation was shown to increase the nuclear accumulation of DDB1 (28). MEFs were infected with adenovirus expressing T7 epitope-tagged DDB1 or a control adenovirus (not shown). Infected cells were subjected to UV or IR (Fig. 2). In wild-type MEFs, UV irradiation caused a significant increase in the nuclear accumulation of DDB1, as judged by a much greater percentage of cells showing both nuclear and cytoplasmic staining for DDB1 compared to that in un-irradiated cells. In DDB2$^{-/-}$ MEFs, no increase in the nuclear accumulation of DDB1 was observed following UV irradiation (Fig. 2), and that is in agreement with defects in the naturally occurring mutant forms of DDB2 (45). IR treatment did not enhance the nuclear accumulation of DDB1; on the other hand, there was a slight inhibition (Fig. 2). It is noteworthy that, in the absence of UV, some cells exhibited nuclear staining for DDB1 and that was not significantly dependent upon DDB2. DDB1 is believed to interact with multiple WD40 repeat proteins (19). It is likely that some of these proteins also are involved in the nuclear accumulation of DDB1 irrespective of UV irradiation.

Differential stability of p53^{S18P} in wild-type versus DDB2$^{-/-}$ MEFs following low-dose UV irradiation. We showed that Cul4A cooperates with MDM2 to enhance the proteolysis of p53 (35). Another group confirmed this observation, indicating that DDB1 also is involved in that process (5). We did not detect any significant difference in the stability of p53 in wild-type versus DDB2$^{-/-}$ MEFs. Itoh et al. (22) studied p53 in DDB2$^{-/-}$ MEFs and reported a twofold lower level of p53 protein in those MEFs compared to that in wild-type MEFs following 6 h of UV irradiation and suggested that the lower level of p53 might be linked to a lack of UV-induced apoptosis in DDB2$^{-/-}$ MEFs. However, those authors did not study the levels of phosphorylated p53 after UV irradiation. UV irradiation activates the DNA damage response pathway of ATR, which phosphorylates p53 at Ser15 in humans and at Ser18 in mice (1, 50, 56). The ATR-mediated phosphorylation at residue Ser18 in mouse p53 does not contribute to the stability of p53, but it stimulates the transcriptional activity of p53 (9). Because DDB2 is significant in the UV-induced nuclear accumulation of DDB1, we investigated whether the Ser18-phos-

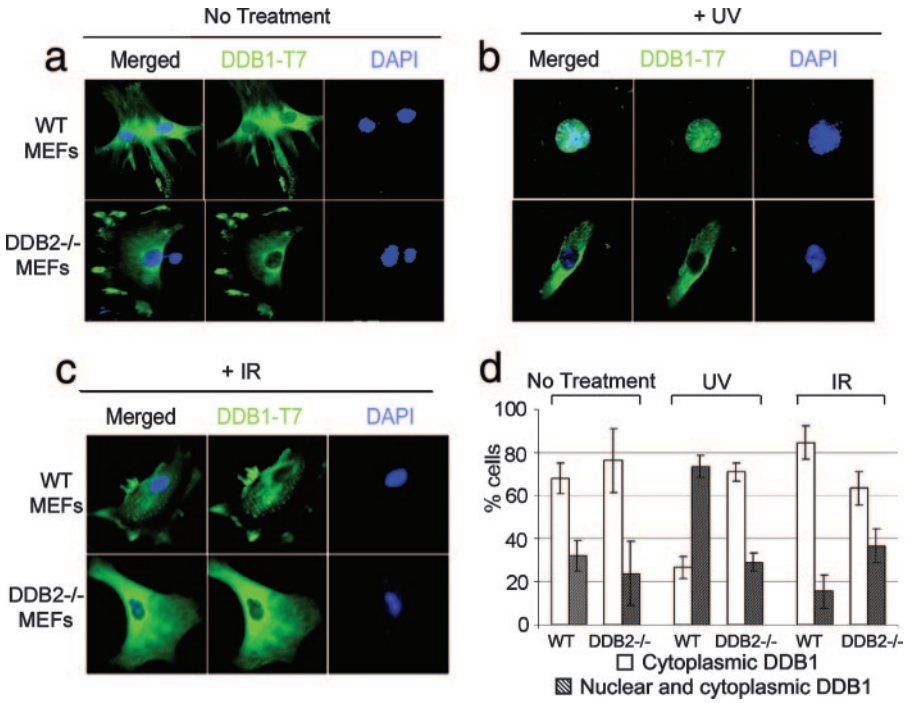

FIG. 2. DDB2$^{-/-}$ MEFs are unresponsive to UV-induced nuclear accumulation of DDB1. MEFs from wild-type (WT) or DDB2$^{-/-}$ embryos were grown on coverslips and infected with adenovirus expressing T7-tagged DDB1. Sixteen hours following infection, the cells were treated with UV irradiation (20 J/m^2) or IR (5 Gy). One hour after irradiation, the cells were fixed and subjected to immunostaining for T7-tagged DDB1 as described in Materials and Methods. We analyzed the localization of DDB1 in 50 to 60 cells, and a quantification of the immunostaining data is shown in panel d.

phorylated form of p53 exhibited differential stability in DDB2$^{-/-}$ MEFs. MEFs from wild-type and DDB2$^{-/-}$ embryos were subjected to UV irradiation (12 J/m^2) and harvested at different time points (0, 1, 3, and 7 h). Extracts of the irradiated cells were analyzed for the level of Ser18-phosphorylated p53 (p53^{S18P}) with a phospho-specific antibody. Interestingly, the DDB2$^{-/-}$ MEFs were found to contain a higher level of p53^{S18P} (Fig. 3a). Similar results were obtained when splenocytes from DDB2$^{-/-}$ or wild-type mice were exposed to UV irradiation (see Fig. S1 in the supplemental material).

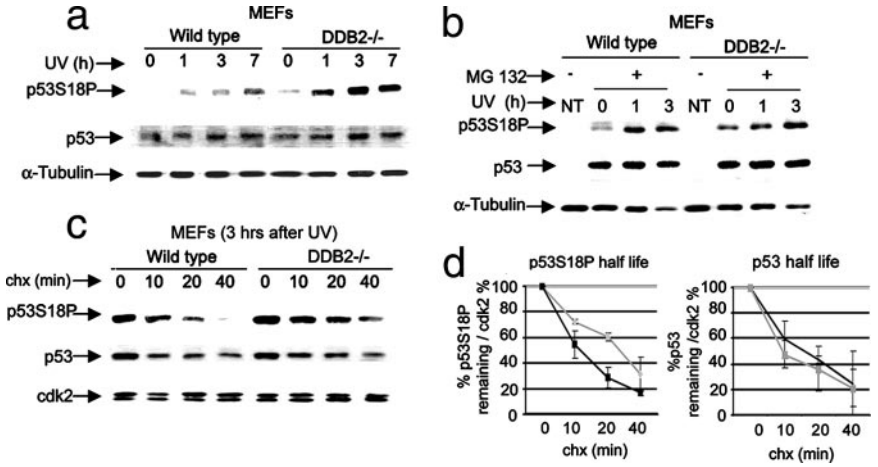

FIG. 3. DDB2-deficient cells are impaired in the proteolysis of p53^{S18P}. MEFs were subjected to UV irradiation (12 J/m^2) and then maintained in the medium for the indicated time periods. Extracts (100 μg) were subjected to Western blot assays. The blots were probed with antibodies against p53^{S18P}, p53, DDB1, and Cdk2 or tubulin. (b) MEFs were treated with MG132 and then irradiated with UV. The UV-irradiated MEFs were maintained in medium for the indicated time periods. Extracts (100 μg) were subjected to Western blot analysis. NT, not treated. (c) MEFs were treated with UV irradiation, and 3 h following irradiation, cycloheximide (chx) was added to the culture medium and the cells were harvested at the indicated time points. The extracts (100 μg) were analyzed by Western blot assays. (d) A quantification of phospho-p53 band intensity is plotted against time after cycloheximide addition. The gray line represents the decay in DDB2$^{-/-}$ MEFs, and the black line represents the decay in wild-type MEFs.

The higher level of $p53^{S18P}$ in $DDB2^{-/-}$ cells could arise from increased phosphorylation by ATR or a deficiency in dephosphorylation. PPM1D phosphatase has been shown to dephosphorylate phospho-p53 and phospho-Chk1 (30). However, the levels of $p53^{S18P}$ in wild-type and $DDB2^{-/-}$ MEFs appeared comparable when the cells were treated with MG132, an inhibitor of the 26S proteasome (Fig. 3b), suggesting that $p53^{S18P}$ is actively degraded by the 26S proteasome in UV-irradiated cells and that $DDB2^{-/-}$ MEFs are deficient in degrading $p53^{S18P}$ following UV irradiation. To confirm a deficiency in the proteolysis of $p53^{S18P}$, we compared the decay rate of $p53^{S18P}$ in wild-type MEFs with that in $DDB2^{-/-}$ MEFs following UV irradiation. MEFs were subjected to UV irradiation, and 3 h later cycloheximide was added to the culture medium. At different time points, the cells were harvested for analysis of the levels of $p53^{S18P}$. Consistent with a deficiency in proteolysis, the $DDB2^{-/-}$ MEFs exhibited a slower decay of $p53^{S18P}$ compared to that in wild-type MEFs (Fig. 3c and d). We did not detect any significant difference in the decay of total p53, suggesting that only a small population of p53 is phosphorylated under the experimental condition (UV irradiation of MEFs at 12 J/m^2) and that DDB2 deficiency does not significantly affect the decay of unphosphorylated p53. The difference in the decay rate of $p53^{S18P}$ is more pronounced at the early time points compared to the later time points (such as 40 min after cycloheximide addition). That could be a result of dephosphorylation of phospho-p53 at later time points (30). Our observation suggests that p53 and $p53^{S18P}$ are degraded by different mechanisms. Moreover, a much shorter half-life of p53 compared to $p53^{S18P}$ in $DDB2^{-/-}$ MEFs is inconsistent with the possibility that $p53^{S18P}$ accumulates as a result of increased phosphorylation in repair-deficient $DDB2^{-/-}$ MEFs. Below, we provide further evidence that accumulation of $p53^{S18P}$ is the cause rather than the effect of the repair deficiency in $DDB2^{-/-}$ MEFs. Also, the repair-deficient cells exhibited increased stabilization of p53 only at later time points (2).

The instability of p53 in UV-irradiated (12 J/m^2) cells in Fig. 3 is apparently in disagreement with the notion that UV irradiation stabilizes p53. We observed only a marginal increase in the steady-state levels of p53 following UV irradiation at 12 J/m^2 (Fig. 4a). In MEFs, robust stabilization could be detected only when high-dose UV irradiation was used (Fig. 4a). The difference in the stability of $p53^{S18P}$ between wild-type and $DDB2^{-/-}$ cells was detected in UV-irradiated cells only. When wild-type and $DDB2^{-/-}$ MEFs were compared following IR, no significant difference in the decay of $p53^{S18P}$ was observed (Fig. 4b). These observations suggest the existence of an active mechanism that induces the proteolysis of $p53^{S18P}$ following low-dose UV irradiation but not following irradiation with a high dose of UV or IR. Moreover, the rapid proteolysis of $p53^{S18P}$ following low-dose UV involves the XP-E gene product DDB2 because $DDB2^{-/-}$ cells are deficient in that process. However, roles of other modifications of p53 could not be ruled out because we analyzed modification only at one site.

To further investigate the mechanism underlying the deficiency of phospho-p53 proteolysis in DDB2-deficient cells, we analyzed the ubiquitination of $p53^{S15P}$. We transfected HeLa cells with a plasmid expressing DDB2 shRNA and isolated clones lacking expression of the DDB2 protein. DDB2 shRNA-expressing cells were transfected with a human Flag-p53 expression plasmid along with a six-His-tagged ubiquitin

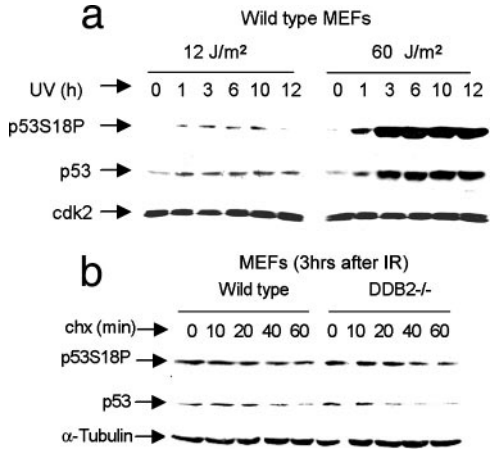

FIG. 4. p53 and $p53^{S18P}$ are unstable specifically in low-dose-UV-irradiated cells. (a) MEFs from wild-type embryos were treated with a low dose (12 J/m^2) or a high dose (60 J/m^2) of UV irradiation and then maintained in the medium for the indicated time period. Extracts (100 μg) of the cells were analyzed for p53 by Western blot assays. (b) MEFs from wild-type or $DDB2^{-/-}$ embryos were treated with IR (5 Gy). After 3 h, cells were treated with cycloheximide (chx) and harvested at the indicated time points. Extracts (100 μg) were analyzed for $p53^{S18P}$ and p53 by Western blot assays.

expression plasmid. The transfected cells were irradiated with UV (12 J/m^2) and treated with MG132. Aliquots of the harvested cells were used to measure transfection efficiency based on Flag-p53 expression (Fig. 5a, left side). The remaining cells were lysed in guanidinium-HCl buffer for purification of the ubiquitinated protein through Ni-nitrilotriacetic acid (NTA)-agarose beads as previously described (53). The eluates from the Ni-NTA-agarose beads were analyzed for ubiquitinated $p53^{S15P}$ with a phospho-p53 antibody and for ubiquitinated p53 with a p53 antibody. As shown in Fig. 5, DDB2 shRNA-expressing cells were significantly deficient in polyubiquitinating $p53^{S15P}$ whereas there was only a marginal difference in the polyubiquitination of total p53. The signals are p53/$p53^{S18P}$ specific, as they were detected only in samples corresponding to transfected cells. Therefore, the DDB2-deficient cells were specifically defective in polyubiquitinating $p53^{S15P}$. We have not ruled out the involvement of other p53 modifications.

$p53^{S18P}$ is a target of the Cul4A-DDB1 pathway. Next, we sought to investigate whether DDB1 or DDB2 functions as an adaptor in targeting $p53^{S18P}$ by the Cul4A-DDB1 ligase. Initially, we studied interactions with epitope-tagged proteins. MEFs from wild-type embryos were infected with an adenovirus that expresses T7 epitope-tagged DDB2 or DDB1. The infected cells were subjected to UV irradiation to generate $p53^{S18P}$ in the presence of MG132 (to stabilize $p53^{S18P}$). Three hours following UV irradiation, the cells were harvested and the extracts were immunoprecipitated with a T7 antibody or a control antibody. The immunoprecipitates were analyzed for the presence of $p53^{S18P}$ with a specific antibody in Western blot assays. $p53^{S18P}$ was detected in the DDB1 immunoprecipitate, but very little $p53^{S18P}$ could be detected in the DDB2 immunoprecipitate (Fig. 6a), suggesting that DDB1 associates with $p53^{S18P}$. We also investigated the interaction with unphosphorylated p53 with higher levels of the extracts because the antibody against total p53 is less sensitive compared to that

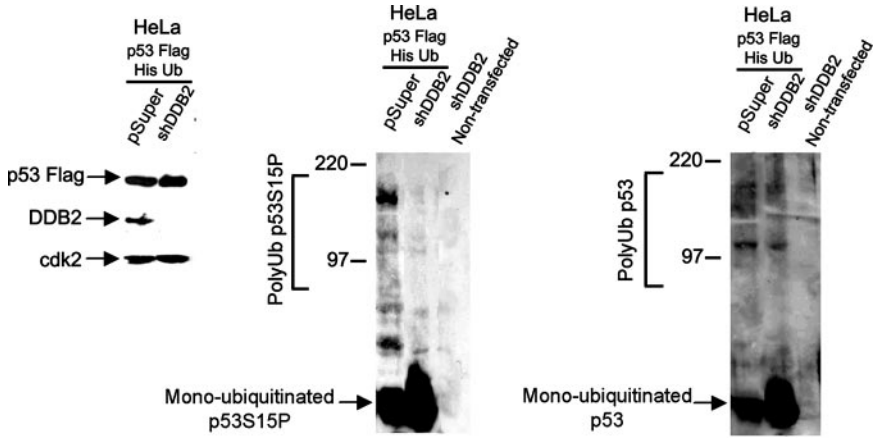

FIG. 5. DDB2 deficiency impedes the ubiquitination of $p53^{S18P}$. HeLa cells expressing DDB2 shRNA or no shRNA (pSuper) were transfected with plasmids expressing Flag-tagged p53 and six-His-tagged ubiquitin (Ub). The transfected cells were treated also with UV irradiation (12 J/m^2) and MG132 (for 5 h). Aliquots (20% of the total) of the transfected cells were analyzed for levels of p53 transgene expression with Flag-tagged antibody and for DDB2 expression with DDB2 antibody (left panel). The remaining aliquots of transfected or untransfected cells were lysed in buffer containing 6 M guanidinium-HCl as previously described (53). The lysates were subjected to Ni-NTA-agarose binding and purification of the ubiquitinated proteins as described in reference 53. The Ni-NTA-agarose-purified fractions were analyzed for ubiquitinated $p53^{S18P}$ and p53 with specific antibodies in Western blot assays. PolyUb, polyubiquitinated.

against $p53^{S18P}$. In those experiments, very little binding was detected when the blot was probed with an antibody against the total p53 protein (Fig. 6b). Following prolonged exposure, a hint of a band could be detected only in the immunoprecipitate from the extracts of UV-irradiated cells (not shown). To further investigate the interaction, we analyzed the interaction between the endogenous proteins. When the extracts from UV-irradiated cells were immunoprecipitated with antibody against $p53^{S18P}$, we did not detect any coprecipitation of DDB1 (not shown). That would be an expected result if DDB1 binding also involves a phosphorylated Ser18 residue in p53. However, when we immunoprecipitated the extracts of UV-irradiated cells with DDB1 antibody, a significant level of $p53^{S18P}$ could be detected coprecipitating with DDB1 (Fig. 6c), further confirming the result obtained with exogenous DDB1. Taken together, our results suggest that DDB1 preferentially binds to $p53^{S18P}$. In these experiments, the roles of other p53 modifications were not considered.

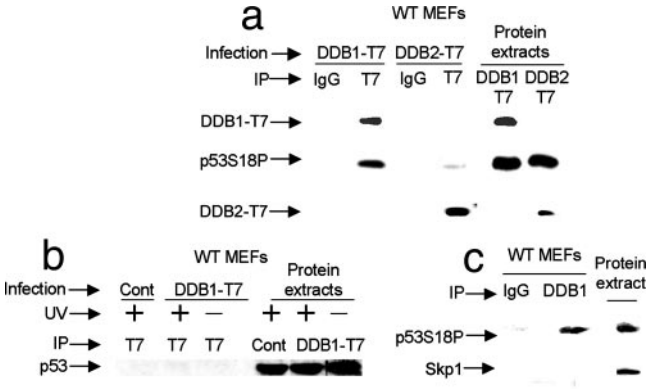

FIG. 6. DDB1 preferentially binds $p53^{S18P}$. (a and b) MEFs from wild-type (WT) embryos were infected with adenovirus expressing T7 epitope-tagged DDB1 or DDB2. Thirteen hours following infection, the cells were treated with MG132 for 2 h and then irradiated with UV (12 J/m^2). Subsequently, the cells were maintained in medium containing MG132 for an additional 3 h. Following that, the cells were harvested and extracts (1.5 mg for the experiments in panel a and 3 mg for the experiments in panel b) of these cells were subjected to immunoprecipitation (IP) with T7 antibody or with isotype-matched immunoglobulin G (IgG). The immunoprecipitates were analyzed for the presence of $p53^{S18P}$ (a) or total p53 (b) by Western blot assay. Total extracts (0.1 mg) were also analyzed for the levels of T7-DDB1, T7-DDB2, $p53^{S18P}$, and total p53. (c) MEFs were UV irradiated in the presence of MG132. Three hours following irradiation, cells were harvested and extracts (2 mg) were subjected to immunoprecipitation with a DDB1 antibody or a control (Cont) antibody. The immunoprecipitates were subjected to Western blot assays with the phopsho-p53 antibody. In this experiment, the blot corresponding to the immunoprecipitate lanes was developed with Fc-horseradish peroxidase (Pierce) instead of a secondary antibody to avoid signals from IgG.

DDB1 functions as an adaptor for Cul4A. Cul4A and DDB1 have been shown to cooperate with Mdm2 in the proteolysis of p53 (5, 35). Therefore, we investigated whether the Cul4A pathway is involved also in the proteolysis of $p53^{S18P}$ following UV irradiation. Cul4A-DDB1 is involved in the proteolysis of Cdt1 (4, 18, 20, 21, 42). Lack of Cdt1 proteolysis in DDB1 knockdown or knockout causes overreplication and activation of the DNA damage response pathway (8, 29). Therefore, we decided to perform gain-of-function experiments. Since $p53^{S18P}$ in wild-type cells is unstable, we studied the effect of Cul4A expression on the stability of $p53^{S18P}$ in $DDB2^{-/-}$ MEFs. Proteolysis of $p53^{S18P}$ occurs in $DDB2^{-/-}$ MEFs, but at a slower rate (Fig. 3d). Those MEFs possess some level of DDB1 in the nucleus (Fig. 2). If the Cul4A pathway is involved, we expected to see an acceleration of proteolysis in those cells upon Cul4A overexpression. The $DDB2^{-/-}$ MEFs were infected with an adenovirus expressing Cul4A or DDB1 or with a control adenovirus. Eighteen hours after infection, the cells were subjected to UV irradiation, and 3 h after irradiation, cycloheximide was added to the culture medium. At different time points following cycloheximide addition, the cells were harvested and the levels of $p53^{S18P}$ were analyzed by

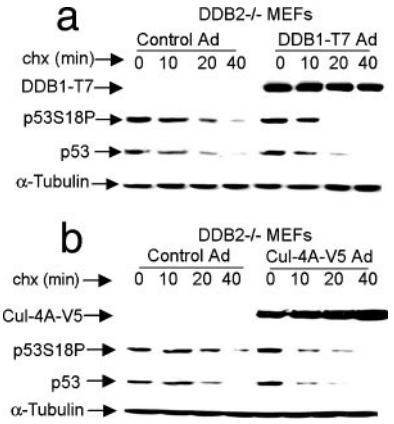

FIG. 7. Cul4A-DDB1 accelerates the decay of $p53^{S18P}$. $DDB2^{-/-}$ MEFs were infected with Cul4A expression adenovirus (Ad), a control adenovirus, or a DDB1 expression virus (b). Fifteen hours after infection, the cells were subjected to UV irradiation (12 J/m^2). Three hours postirradiation, the cells were treated with cycloheximide (chx) for the indicated time periods. Extracts (100 μg) of the cells were analyzed for the levels of $p53^{S18P}$ by Western blot experiments.

Western blot assays. Clearly, expression of Cul4A accelerated the decay rates of both p53 and $p53^{S18P}$ (Fig. 7). The accelerated decay of p53 is consistent with previous reports (5, 35). The accelerated decay of $p53^{S18P}$ suggests that Cul4A is involved also in the proteolysis of $p53^{S18P}$. Some acceleration was observed also in cells expressing DDB1 (Fig. 7). Since $DDB2^{-/-}$ MEFs possess some level of DDB1 in the nucleus, we think that Cul4A associates with the available DDB1 in the nucleus to increase the decay of $p53^{S18P}$.

$DDB2^{-/-}$ MEFs express $p21^{Waf1/Cip1}$ at a high level following low-dose UV irradiation. The Ser18-phosphorylated form of p53 is transcriptionally more active, and a deficiency in its turnover is expected to cause greater accumulation of the target genes, such as that for $p21^{Waf1/Cip1}$. $p21^{Waf1/Cip1}$ was shown to be unstable in UV-irradiated cells (7). However, a recent study indicated that the steady-state level of $p21^{Waf1/Cip1}$ does not change significantly during the first several hours following UV irradiation (12 J/m^2) (23). The lack of an increase in $p21^{Waf1/Cip1}$ following UV irradiation (12 J/m^2) is consistent with the quick decay of $p53^{S18P}$ observed in our experiments (Fig. 3). Because the $DDB2^{-/-}$ MEFs accumulated $p53^{S18P}$, we compared the mRNA levels of $p21^{Waf1/Cip1}$ by quantitative real-time PCR. Consistent with previous observations (23), we did not notice any significant change in the level of $p21^{Waf1/Cip1}$ in wild-type MEFs in the first few hours following UV irradiation (Fig. 8a). $DDB2^{-/-}$ MEFs, on the other hand, exhibited an increase in the levels of $p21^{Waf1/Cip1}$ mRNA following UV irradiation (Fig. 8a). The increased expression of $p21^{Waf1/Cip1}$ in UV-irradiated $DDB2^{-/-}$ MEFs is consistent with higher levels of $p53^{S18P}$ in those cells. Increased expression was also detected at the protein level (Fig. 8a). Interestingly, we also observed stabilization of $p21^{Waf1/Cip1}$ protein in $DDB2^{-/-}$ MEFs (our unpublished observation). Increased expression of $p21^{Waf1/Cip1}$ mRNA was observed in HeLa cells lacking DDB2 as well. We generated a stable line of HeLa cells expressing shRNA against DDB2 (Fig. 5). Those cells, upon low-dose UV irradiation, exhibited increased stability of $p53^{S18P}$, and they expressed $p21^{Waf1/Cip1}$ mRNA at a higher level compared to a control line (Fig. 8b). The increased expression of $p21^{Waf1/Cip1}$ mRNA in those cells is dependent upon p53 because knockdown of p53 eliminated the UV-induced expression of the $p21^{Waf1/Cip1}$ mRNA (Fig. 8c).

Reduction or elimination of $p21^{Waf1/Cip1}$ reverses the repair deficiency in $DDB2^{-/-}$ MEFs. p53 is required for NER (15, 47), but the link between $p21^{Waf1/Cip1}$ and NER is controversial. It is commonly believed that $p21^{Waf1/Cip1}$ slows down cell cycle progression to allow time for repair. Consistent with that notion, in human colon cancer cells it was shown to play a positive role in repair (32). In primary MEFs, on the other hand, $p21^{Waf1/Cip1}$ is not required for NER (47). Interestingly, two studies indicated that an increased level of $p21^{Waf1/Cip1}$ inhibits NER through inhibition of PCNA, which is required for repair synthesis (12, 38). Other in vitro studies detected inhibition of repair synthesis by $p21^{Waf1/Cip1}$ only under specific conditions (44). A recent study demonstrated that $Gadd45^{-/-}$ keratinocytes accumulated $p21^{Waf1/Cip1}$ and that deletion of $p21^{Waf1/Cip1}$ reversed the NER deficiency (31). Therefore, we decided to examine whether the accumulation of $p21^{Waf1/Cip1}$ in a $DDB2^{-/-}$ background was responsible for the reduced UDS observed in Fig. 1.

To investigate the role of $p21^{Waf1/Cip1}$, we used a lentivirus expressing $p21^{Waf1/Cip1}$ shRNA to knock down the levels of $p21^{Waf1/Cip1}$ in UV-irradiated $DDB2^{-/-}$ MEFs. MEFs were infected with the $p21^{Waf1/Cip1}$ shRNA expression virus or a control lentivirus. Infected cells were subjected to UV irradiation and processed for UDS (47). An aliquot of infected cells was also analyzed for a reduction in the level of $p21^{Waf1/Cip1}$. The shRNA caused only a twofold reduction in the level of $p21^{Waf1/Cip1}$; a quantification of the $p21^{Waf1/Cip1}$ level is shown in Fig. 9a. Nevertheless, the twofold reduction in the level of $p21^{Waf1/Cip1}$ was sufficient to cause a significant increase in UDS in $DDB2^{-/-}$ MEFs (Fig. 9b). A greater number of nuclei exhibited a higher number of grains in $p21^{Waf1/Cip1}$ knockdown cells compared to the control, suggesting that accumulation of $p21^{Waf1/Cip1}$ in $DDB2^{-/-}$ MEFs contributes to the repair deficiency in those cells.

To obtain further genetic evidence, we crossed $DDB2^{-/-}$ mice with $p21^{Waf1/Cip1-/-}$ mice to generate a double-knockout strain. MEFs derived from the double-knockout strain were compared with those from the single-knockout strains for UDS activity following UV irradiation. As expected from previous studies (47), $p21^{Waf1/Cip1-/-}$ MEFs exhibited levels of UDS comparable to those of wild-type MEFs (Fig. 10). $DDB2^{-/-}$ MEFs exhibited lower levels of UDS, as there were more nuclei with fewer grains. The MEFs from the double-knockout embryo exhibited UDS at the wild-type level (Fig. 10), confirming the notion that increased accumulation of $p21^{Waf1/Cip1}$ is responsible for the repair deficiency in $DDB2^{-/-}$ MEFs.

DISCUSSION

The work presented here is significant in several ways. Using mouse models, we provide genetic evidence for a new mechanism by which DDB2 participates in NER. In low-dose-UV-irradiated cells, DDB2 plays an important role in down-regulating the levels of $p53^{S18P}$ by stimulating the nuclear import of DDB1, which enhances proteolysis of $p53^{S18P}$. The proteolysis of $p53^{S18P}$ is important in maintaining expression of $p21^{Waf1/Cip1}$ at a low level

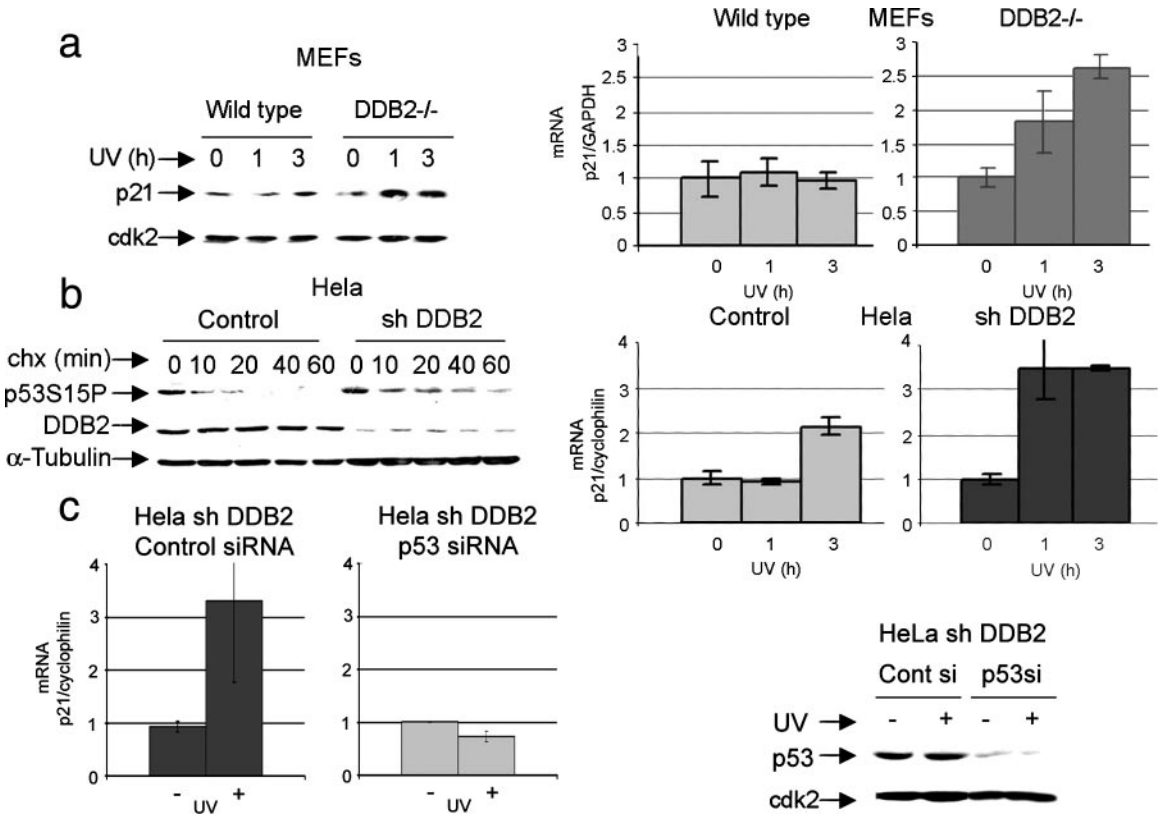

FIG. 8. Increased expression of p21Cip1 in DDB2$^{-/-}$ MEFs or DDB2-deficient HeLa cells following UV irradiation. Wild-type or DDB2$^{-/-}$ MEFs (a) were subjected to UV irradiation (12 J/m^2) and then maintained in 10% fetal bovine serum medium for the indicated time periods. (Right) Total RNA was analyzed by quantitative real-time PCR for the levels of p21$^{Waf1/Cip1}$ mRNA as described in Materials and Methods. Extracts (50 μg) were subjected to Western blot assays. The blots were probed with antibodies against p21Cip1 and Cdk2 (left). (b) HeLa cells were transfected with empty vector (control) or vector expressing DDB2 shRNA to isolate stable clones. Cells were treated with UV irradiation at 12 J/m^2. Three hours following UV irradiation, cycloheximide (chx) was added to block new protein synthesis. At the indicated time points, cells were harvested and extracts were assayed for p53^{S18P} (left). (Right) Total RNA from the HeLa cells after UV irradiation was subjected to quantitative real-time PCR to assay the levels of p21$^{Waf1/Cip1}$ mRNA. (c) HeLa cells expressing DDB2 shRNA were transfected with control (Cont) siRNA or p53 siRNA. The transfected cells were treated with UV irradiation. Three hours following UV treatment, cells were harvested and total RNAs were subjected to quantitative real-time PCR for the levels of p21$^{Waf1/Cip1}$ mRNA.

to support efficient NER. We suggest that accumulation of p53^{S18P} is the cause of the repair deficiency in DDB2$^{-/-}$ cells because elimination of p21$^{Waf1/Cip1}$, which is a critical downstream target of p53^{S18P}, reverses the deficiency.

Stability of p53/p53^{S18P} in UV-irradiated MEFs. DNA-damaging agents, including UV irradiation, were shown to stabilize p53 by phosphorylating p53 at the Mdm2-binding site through the activation of ATM/ATR and the checkpoint kinases (reviewed in reference 50). However, recent studies with phosphorylation-defective mutants in mouse knock-in models have challenged that view (49 and references therein). In this study, we analyzed the stability of p53 and p53^{S18P} in MEFs. One major caveat of our analyses arises from the fact that p53 is modified extensively and we assayed only total p53 and p53^{S18P}. Therefore, we could not rule out contributions of other modifications in our study. We observed that a low dose of UV irradiation (12 J/m^2) does not cause significant stabilization of p53 or p53^{S18P} at the early time points. The stabilization was seen in MEFs when treated with high-dose UV irradiation (60 J/m^2). Therefore, the mechanisms that stabilize p53 are active only in high-dose-UV-irradiated cells. We observed phosphorylation of p53 within 1 h at the Ser18 residue, a site phosphorylated by the ATM/ATR kinases, following low-dose UV irradiation. In the wild-type MEFs, Ser18-phosphorylated p53 was as unstable as p53 (Fig. 3). That is consistent with the previous finding that phosphorylation at Ser18 is insufficient for stabilization of p53 (9). Treatment with a proteasome inhibitor stabilized both p53 and p53^{S18P} (Fig. 3). Previous studies suggested that, following the repair of UV- and IR-induced DNA damage, phospho-p53 is dephosphorylated by PPM1D phosphatase (30). Our observations suggest the existence of an additional active mechanism involving the ubiquitin-proteasome pathway that eliminates p53^{S18P} in low-dose-UV-irradiated cells.

In DDB2$^{-/-}$ MEFs, on the other hand, a form of p53 containing phosphorylation at Ser18 (p53^{S18P}) accumulated, resulting from increased stability. The accumulation of p53^{S18P} was associated with an increase in the expression of p21$^{Waf1/Cip1}$, confirming the presence of higher levels of active p53 in DDB2$^{-/-}$ MEFs. The accumulation of p53^{S18P} in UV-irradiated DDB2$^{-/-}$ MEFs could be explained also by continued phosphorylation in repair-deficient cells. However, the kinetics

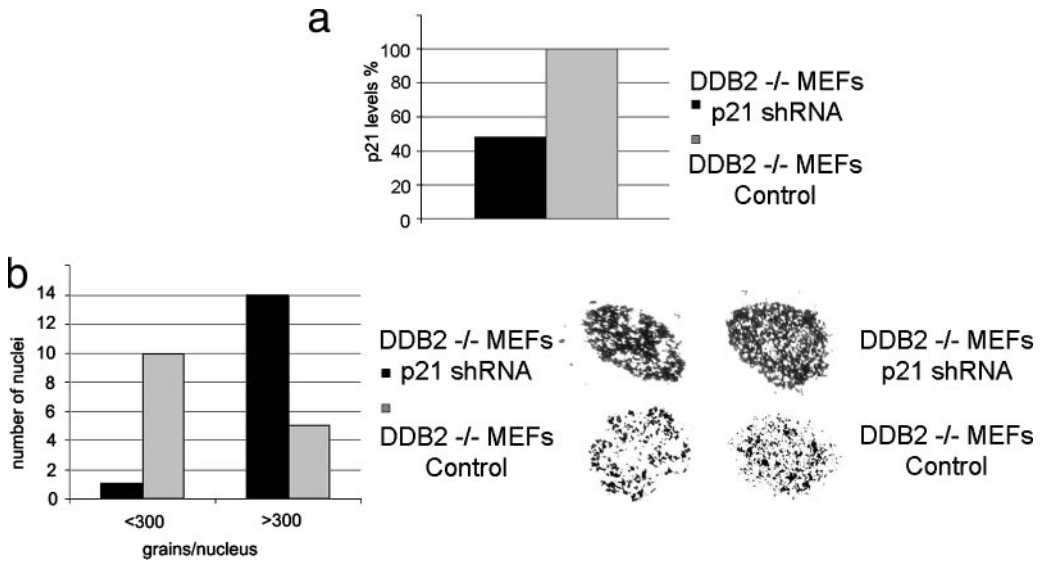

FIG. 9. Repair deficiency in DDB2$^{-/-}$ MEFs is reversed by partial depletion of p21$^{Waf1/Cip1}$. DDB2$^{-/-}$ MEFs were infected with lentivirus expressing shRNA against p21$^{Waf1/Cip1}$ or a control shRNA. Three days following infection, part of the infected cells were subjected to a Western blot assay with an antibody against p21$^{Waf1/Cip1}$ or tubulin (loading control). Relative levels of p21Cip1 were quantified, and the results are shown in panel a. The rest of the infected cells were subjected to UDS assays, and the numbers of grains per nucleus from 15 nuclei are plotted in panel b.

of accumulation of p53^{S18P} is quite rapid. It was shown that repair-deficient cells exhibited increased stabilization of p53 only at later time points (2). Moreover, the levels of p53^{S18P} were comparable between wild-type and DDB2$^{-/-}$ MEFs in the presence of a proteasome inhibitor. We did not observe a huge increase in the level of p53^{S18P} in DDB2$^{-/-}$ MEFs in the presence of MG132 (Fig. 3b), which would be expected from continued phosphorylation in repair-deficient cells. Also, we observed that in DDB2$^{-/-}$ MEFs, the half-life of p53^{S18P} was much longer than that of total p53 (Fig. 3c), suggesting that they are degraded through different pathways. Furthermore, we show that deletion of p21$^{Waf1/Cip1}$, a major downstream target of p53^{S18P}, reverses the repair deficiency in DDB2$^{-/-}$ MEFs, providing evidence that accumulation of p53^{S18P} is the cause rather than the effect of repair deficiency. Our observations are clearly congruent with the notion that p53^{S18P} is actively degraded in low-dose-UV-irradiated cells and that there is a deficiency in the proteolysis of p53^{S18P} in DDB2$^{-/-}$ MEFs.

Phospho-p53 is a target of the Cul4A-DDB1 ligase. We showed that Cul4A could target p53 for proteolysis. Moreover, expression of Cul4A delayed the accumulation of p53 following UV irradiation (35). Interestingly, the Cul4A-mediated proteolysis of p53 is dependent upon Mdm2 because Cul4A

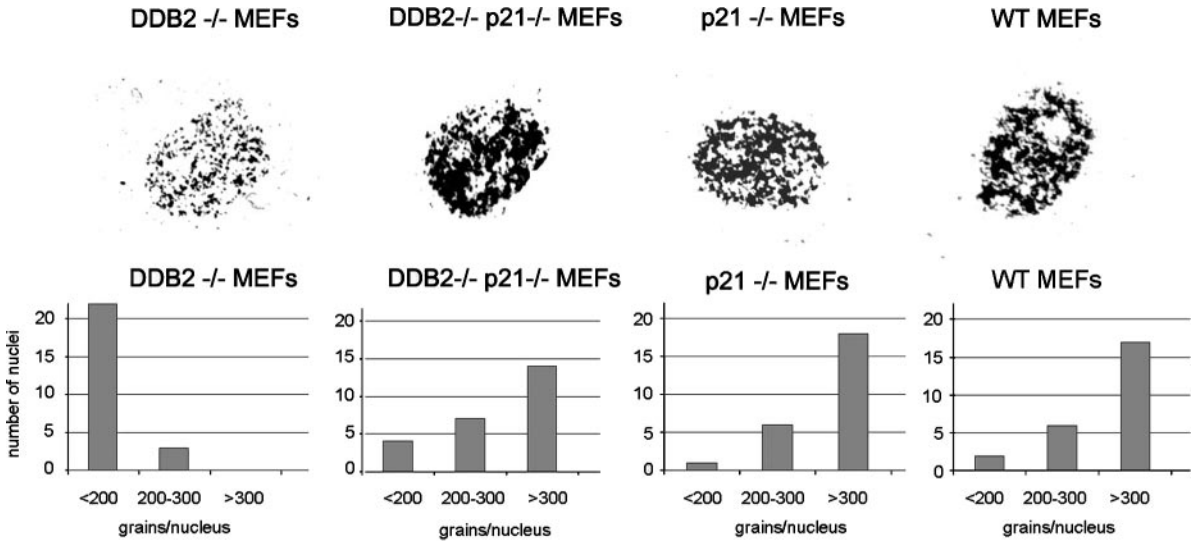

FIG. 10. Deletion of the gene for p21$^{Waf1/Cip1}$ reverses the repair deficiency in DDB2$^{-/-}$ MEFs. MEFs from wild-type (WT), DDB2$^{-/-}$, p21$^{-/-}$, and DDB2$^{-/-}$ p21$^{-/-}$ embryos were subjected to UDS analyses as described in Materials and Methods. After quantification, the numbers of grains per nucleus were plotted. Representative nuclei are shown.

failed to enhance the decay of p53 in p53/Mdm2$^-$ MEFs. Moreover, Cul4A-mediated proteolysis is inhibited by ARF, an inhibitor of Mdm2 (35). Since Cul4A associates with Mdm2, we think that Cul4A functions as a cofactor for Mdm2-mediated proteolysis of p53. It is noteworthy that Cul4A remains associated with the COP9 signalosome, which was shown to associate with p53/Mdm2 and play a role in the proteolysis of p53 (6). It is possible that Cul4A enhances the signalosome pathway of proteolysis of p53. Another group confirmed our results (5), providing additional evidence of a role for DDB1 in the Cul4A/Mdm2-mediated proteolysis of p53. In this study, we showed that DDB1 preferentially bound to p53 that is phosphorylated at Ser18. Moreover, expression of Cul4A accelerated the decay of p53 phosphorylated at Ser18. These results suggest that DDB1 allows the targeting of p53^{S18P} by Cul4A. Interestingly, the nuclear accumulation of DDB1 is enhanced by UV irradiation requiring DDB2 (Fig. 2). Therefore, we suggest that the delay in the proteolysis of p53^{S18P} in DDB2$^{-/-}$ MEFs is a result of a lower level of DDB1 in the nucleus compared to that in UV-irradiated wild-type MEFs, as p53^{S18P} is believed to be a nuclear protein. Our observations provide insight into the mechanism by which p53^{S18P} is targeted for proteolysis in low-dose-UV-irradiated cells. It is noteworthy that phospho-Chk1 has been shown to be a target of proteolysis involving Cul4A following genotoxic stress (55).

p21$^{Waf1/Cip1}$ and NER in UV-irradiated cells. p21$^{Waf1/Cip1}$ is not required for NER, as cells lacking p21$^{Waf1/Cip1}$ carry out NER efficiently following UV irradiation (47). However, because p21$^{Waf1/Cip1}$ binds PCNA, a factor required for both NER and DNA replication (37), several groups have investigated the possibility of inhibitory effects of p21$^{Waf1/Cip1}$ on NER. Initial studies by Li et al. (27) and Shivji et al. (43), with in vitro assay systems for both excision and resynthesis steps, did not find any inhibitory effect of p21$^{Waf1/Cip1}$ on NER. Pan et al. (38), on the other hand, observed significant inhibition of both excision and resynthesis by p21$^{Waf1/Cip1}$ by using similar in vitro assays. In their assays, resynthesis was more sensitive to inhibition by p21$^{Waf1/Cip1}$ than was excision. Moreover, a peptide corresponding to the C-terminal residues of p21$^{Waf1/Cip1}$ that binds to PCNA was able to inhibit NER in vitro (38). The apparent discrepancy in the observations could have resulted from differences in the extracts used in the assays. For example, excess cyclin-cdk in the extracts would sequester p21$^{Waf1/Cip1}$, blocking its interaction with PCNA. Interestingly, later studies by Shivji et al. (44) indicated that prebinding of p21$^{Waf1/Cip1}$ with PCNA could inhibit the filling of a 30-nucleotide gap, a model for the resynthesis step of NER, by purified DNA polymerases ∂ and ε. That study also confirmed that a synthetic PCNA-binding p21$^{Waf1/Cip1}$ peptide is an efficient inhibitor of NER. The inhibition of NER by the C-terminal PCNA-binding domain of p21$^{Waf1/Cip1}$ was further confirmed by both in vitro and in vivo experiments by Cooper et al. (12). It is possible that the C-terminal peptide of p21$^{Waf1/Cip1}$ dissected away the interference from cyclin-cdk (which binds to the N-terminal region of p21$^{Waf1/Cip1}$), allowing the inhibition of NER to be easily detectable. In vivo accumulation of endogenous p21$^{Waf1/Cip1}$ also inhibits NER. A recent report indicated that Gadd45$^{-/-}$ keratinocytes accumulate p21$^{Waf1/Cip1}$ at a high level and that the cells are deficient in NER. Moreover, deletion of p21$^{Waf1/Cip1}$ restores NER capacity to Gadd45-deficient keratinocytes (31). These results are different from what was observed in MEFs, in which deletion of p21$^{Waf1/Cip1}$ in the Gadd45$^{-/-}$ background did not increase repair function (47). To explain the discrepancy, Maeda et al. (31) stated that, unlike Gadd45$^{-/-}$ keratinocytes, Gadd45$^{-/-}$ MEFs did not accumulate p21$^{Waf1/Cip1}$ (31). In our present study, we consistently observed that DDB2$^{-/-}$ MEFs expressed p21$^{Waf1/Cip1}$ at a higher level compared to wild-type MEFs following UV irradiation, an observation that is expected from an accumulation of p53^{S18P} in those cells. Therefore, we considered a potential role for high-level p21$^{Waf1/Cip1}$ in the inhibition of NER in DDB2$^{-/-}$ MEFs.

We observed that shRNA-mediated knockdown of the p21$^{Waf1/Cip1}$ level by 50% caused a huge increase in repair synthesis in DDB2$^{-/-}$ MEFs, suggesting that the increased expression of p21$^{Waf1/Cip1}$ in DDB2$^{-/-}$ MEFs was responsible for the reduced level of UDS. These results were further confirmed by generating DDB2$^{-/-}$ p21$^{-/-}$ double-knockout mice. The MEFs from the double-knockout embryos, unlike those from DDB2$^{-/-}$ embryos, exhibited wild-type levels of UDS. Our results suggest that the regulation of the mechanism that stimulates the synthesis of p21$^{Waf1/Cip1}$ is critical for efficient NER. We propose that by actively degrading p53^{S18P}, Cul4A-DDB1 and DDB2 maintain the synthesis of p21$^{Waf1/Cip1}$ at a level that supports efficient repair synthesis. We think that by enhancing DDB2-mediated nuclear import of DDB1, UV irradiation causes an increase in the Cul4A-DDB1-DDB2 complex bound to damaged chromatin. As suggested by others, chromatin-bound Cul4A-DDB1-DDB2 may have a role in histone modification and XP-C recruitment. We see damaged-chromatin binding as a mechanism also to ensure nuclear accumulation of the active ligase. Subsequent proteolysis of DDB2 (3, 14, 33) releases Cul4A-DDB1 from damaged DNA, allowing it to target p53^{S18P}. Because p21$^{Waf1/Cip1}$ is believed to be an inhibitor of repair synthesis, we suggest that, in addition to its potential role in CPD excision, DDB2 plays an important role in repair synthesis.

ACKNOWLEDGMENT

This work was supported by grants from the NIH (CA 77637 and AG 024138) to P.R.

We thank H. Kiyokawa, Northwestern University, for the p21 shRNA-expressing lentivirus.

REFERENCES

1. **Abraham, R. T.** 2001. Cell cycle checkpoint signaling through the ATM and ATR kinases. Genes Dev. **15:**2177–2196.
2. **Abrahams, P. J., R. Schouten, T. van Laar, A. Houweling, C. Terleth, and A. J. van der Eb.** 1995. Different regulation of p53 stability in UV-irradiated normal and DNA repair deficient human cells. Mutat. Res. **336:**169–180.
3. **Alekseev, S., H. Kool, H. Rebel, M. Fousteri, J. Moser, C. Backendorf, F. R. de Gruijl, H. Vrieling, and L. H. Mullenders.** 2005. Enhanced DDB2 expression protects mice from carcinogenic effects of chronic UV-B irradiation. Cancer Res. **65:**10298–10306.
4. **Arias, E. E., and J. C. Walter.** 2006. PCNA functions as a molecular platform to trigger Cdt1 destruction and prevent re-replication. Nat. Cell Biol. **8:** 84–90.
5. **Banks, D., M. Wu, L. A. Higa, J. Quan, T. Ye, R. Kobayashi, H. Sun, and H. Zhang.** 2006. L2DTL/CDT2 and PCNA interact with p53 and regulate p53 polyubiquitination and protein stability through MDM2 and CUL4A/DDB1 complex. Cell Cycle **5:**1719–1729.
6. **Bech-Otschir, D., R. Kraft, X. Huang, P. Henklein, B. Kapelari, C. Pollmann, and W. Dubiel.** 2001. COP9 signalosome-specific phosphorylation targets p53 to degradation by the ubiquitin system. EMBO J. **20:**1630–1639.
7. **Bendjennat, M., J. Boulaire, T. Jascur, H. Brickner, V. Barbier, A. Sarasin, A. Fotedar, and R. Fotedar.** 2003. UV irradiation triggers ubiquitin-dependent degradation of p21^{WAF1} to promote DNA repair. Cell **114:**599–610.

8. **Cang, Y., J. Zhang, S. A. Nicholas, J. Bastien, B. Li, P. Zhou, and S. P. Goff.** 2006. Deletion of DDB1 in mouse brain and lens leads to p53-dependent elimination of proliferating cells. Cell **127:**929–940.
9. **Chao, C., M. Hergenhahn, M. D. Kaeser, Z. Wu, S. Saito, R. Iggo, M. Hollstein, E. Appella, and Y. Xu.** 2003. Cell type- and promoter-specific roles of Ser18 phosphorylation in regulating p53 responses. J. Biol. Chem. **278:** 41028–41033.
10. **Chen, X., J. Zhang, J. Lee, P. S. Lin, J. M. Ford, N. Zheng, and P. Zhou.** 2006. A kinase-independent function of c-Abl in promoting proteolytic destruction of damaged DNA binding proteins. Mol. Cell **22:**489–499.
11. **Cleaver, J. E.** 2005. Cancer in xeroderma pigmentosum and related disorders of DNA repair. Nat. Rev. Cancer **5:**564–573.
12. **Cooper, M. P., A. S. Balajee, and V. A. Bohr.** 1999. The C-terminal domain of p21 inhibits nucleotide excision repair in vitro and in vivo. Mol. Biol. Cell **10:**2119–2129.
13. **Datta, A., S. Bagchi, A. Nag, P. Shiyanov, G. R. Adami, T. Yoon, and P. Raychaudhuri.** 2001. The p48 subunit of the damaged-DNA binding protein DDB associates with the CBP/p300 family of histone acetyltransferase. Mutat. Res. **486:**89–97.
14. **El-Mahdy, M. A., Q. Zhu, Q. E. Wang, G. Wani, M. Praetorius-Ibba, and A. A. Wani.** 2006. Cullin 4A-mediated proteolysis of DDB2 protein at DNA damage sites regulates in vivo lesion recognition by XPC. J. Biol. Chem. **281:**13404–13411.
15. **Ford, J. M., and P. Hanawalt.** 1997. Expression of wild-type p53 is required for efficient global genomic nucleotide excision repair in UV-irradiated human fibroblasts. J. Biol. Chem. **272:**28073–28080.
16. **Friedberg, E. C.** 2001. How nucleotide excision repair protects against cancer. Nat. Rev. Cancer **1:**22–33.
17. **Groisman, R., J. Polanowska, I. Kuraoka, J. Sawada, M. Saijo, R. Drapkin, A. F. Kisselev, K. Tanaka, and Y. Nakatani.** 2003. The ubiquitin ligase activity in the DDB2 and CSA complexes is differentially regulated by the COP9 signalosome in response to DNA damage. Cell **113:**357–367.
18. **Higa, L. A., I. S. Mihaylov, D. P. Banks, J. Zheng, and H. Zhang.** 2003. Radiation-mediated proteolysis of CDT1 by CUL4-ROC1 and CSN complexes constitutes a new checkpoint. Nat. Cell Biol. **5:**1008–1015.
19. **Higa, L. A., M. Wu, T. Ye, R. Kobayashi, H. Sun, and H. Zhang.** 2006. CUL4-DDB1 ubiquitin ligase interacts with multiple WD40-repeat proteins and regulates histone methylation. Nat. Cell Biol. **8:**1277–1283.
20. **Hu, J., C. M. McCall, T. Ohta, and Y. Xiong.** 2004. Targeted ubiquitination of Cdt1 by the DDB1-Cul4A-Roc1 ligase in response to DNA damage. Nat. Cell Biol. **6:**1003–1009.
21. **Hu, J., and Y. Xiong.** 2006. An evolutionarily conserved function of proliferating cell nuclear antigen for Cdt1 degradation by the Cul4-Ddb1 ubiquitin ligase in response to DNA damage. J. Biol. Chem. **281:**3753–3756.
22. **Itoh, T., D. Cado, R. Kamide, and S. Linn.** 2004. DDB2 gene disruption leads to skin tumors and resistance to apoptosis after exposure to ultraviolet light but not a chemical carcinogen. Proc. Natl. Acad. Sci. USA **101:**2052–2057.
23. **Itoh, T., and S. Linn.** 2005. The fate of p21CDKN1A in cells surviving UV-irradiation. DNA Repair **4:**1457–1462.
24. **Kapetanaki, M. G., J. Guerrero-Santoro, D. C. Bisi, C. L. Hsieh, V. Rapic-Otrin, and A. S. Levine.** 2006. The DDB1-CUL4ADDB2 ubiquitin ligase is deficient in xeroderma pigmentosum group E and targets histone H2A at UV-damaged DNA sites. Proc. Natl. Acad. Sci. USA **103:**2588–2593.
25. **Keeney, S., A. P. Eker, T. Brody, W. Vermeulen, D. Bootsma, J. H. Hoeijmakers, and S. Linn.** 1994. Correction of the DNA repair defect in xeroderma pigmentosum group E by injection of a DNA damage-binding protein. Proc. Natl. Acad. Sci. USA **91:**4053–4056.
26. **Kulaksiz, G., J. T. Reardon, and A. Sancar.** 2005. Xeroderma pigmentosum complementation group E protein (XPE/DDB2): purification of various complexes of XPE and analyses of their damaged DNA binding and putative DNA repair properties. Mol. Cell. Biol. **25:**9784–9792.
27. **Li, R., S. Waga, G. J. Hannon, D. Beach, and B. Stillman.** 1994. Differential effects by the p21 CDK inhibitor on PCNA-dependent DNA replication and repair. Nature **371:**534–537.
28. **Liu, W., A. F. Nichols, J. A. Graham, R. Dualan, A. Abbas, and S. Linn.** 2000. Nuclear transport of human DDB protein induced by ultraviolet light. J. Biol. Chem. **275:**21429–21434.
29. **Lovejoy, C. A., K. Lock, A. Yenamandra, and D. Cortez.** 2006. DDB1 maintains genome integrity through regulation of Cdt1. Mol. Cell. Biol. **26:**7977–7990.
30. **Lu, X., B. Nannenga, and L. A. Donehower.** 2005. PPM1D dephosphorylates Chk1 and p53 and abrogates cell cycle checkpoints. Genes Dev. **19:**1162–1174.
31. **Maeda, T., R. A. Espino, E. G. Chomey, L. Luong, A. Bano, D. Meakins, and V. A. Tron.** 2005. Loss of $p21^{Waf1/Cip1}$ in Gadd45-deficient keratinocytes restores DNA repair capacity. Carcinogenesis **26:**1804–1810.
32. **McDonald, E. R., III, G. S. Wu, T. Waldman, and W. S. El-Diery.** 1996. Repair defect in $p21^{Waf1/Cip1-/-}$ human cancer cells. Cancer Res. **56:**2250–2256.
33. **Nag, A., T. Bondar, S. Shiv, and P. Raychaudhuri.** 2001. The XP-E gene product DDB2 is a specific target of cullin 4A in mammalian cell. Mol. Cell. Biol. **21:**6738–6747.
34. **Nag, A., A. Datta, K. Yoo, D. Bhattacharyya, A. Chakrabortty, X. Wang, B. L. Slagle, R. H. Costa, and P. Raychaudhuri.** 2001. DDB2 induces nuclear accumulation of the hepatitis B virus X protein independently of binding to DDB1. J. Virol. **75:**10383–10389.
35. **Nag, A., S. Bagchi, and P. Raychaudhuri.** 2004. Cul4A physically associates with MDM2 and participates in the proteolysis of p53. Cancer Res. **64:**8152–8165.
36. **Nichols, A. F., T. Itoh, J. A. Graham, W. Liu, M. Yamaizumi, and S. Linn.** 2000. Human damage-specific DNA-binding protein p48. Characterization of XPE mutations and regulation following UV irradiation. J. Biol. Chem. **275:**21422–21428.
37. **Nichols, A. F., and A. Sancar.** 1992. Purification of PCNA as a nucleotide excision repair protein. Nucleic Acids Res. **20:**2441–2446.
38. **Pan, Z. Q., J. T. Reardon, Li, L., H. Flores-Rozas, R. Legerski, A. Sancar, and J. Hurwitz.** 1995. Inhibition of nucleotide excision repair by the cyclin-dependent kinase inhibitor p21. J. Biol. Chem. **270:**22008–22016.
39. **Rapi ć Otrin, V., I. Kuraoka, T. Nardo, M. McLenigan, A. P. Eker, M. Stefanini, A. S. Levine, and R. D. Wood.** 1998. Relationship of the xeroderma pigmentosum group E DNA repair defect to the chromatin and DNA binding proteins UV-DDB and replication protein A. Mol. Cell. Biol. **18:**3182–3190.
40. **Reardon, J. T., and A. Sancar.** 2003. Recognition and repair of the cyclobutane thymine dimer, a major cause of skin cancers, by the human excision nuclease. Genes Dev. **17:**2539–2551.
41. **Sancar, A., L. A. Lindsey-Boltz, K. Unsal-Kacmaz, and S. Linn.** 2004. Molecular mechanisms of mammalian DNA repair and the DNA damage checkpoints. Annu. Rev. Biochem. **73:**39–85.
42. **Senga, T., U. Sivaprasad, W. Zhu, J. H. Park, E. E. Arias, J. C. Walter, and A. Dutta.** 2006. PCNA is a cofactor for Cdt1 degradation by CUL4/DDB1-mediated N-terminal ubiquitination. J. Biol. Chem. **281:**6246–6252.
43. **Shivji, M. K., S. J. Grey, U. P. Strausfeld, R. D. Wood, and J. J. Blow.** 1994. Cip1 inhibits DNA replication but not PCNA-dependent nucleotide excision-repair. Curr. Biol. **4:**1062–1068.
44. **Shivji, M. K., E. Ferrari, K. Ball, U. Hubscher, and R. D. Wood.** 1998. Resistance of human nucleotide repair synthesis in vitro to p21Cdn1. Oncogene **17:**2827–2838.
45. **Shiyanov, P., S. A. Hayes, M. Donepudi, A. F. Nichols, S. Linn, B. L. Slagle, and P. Raychaudhuri.** 1999. The naturally occurring mutants of DDB are impaired in stimulating nuclear import of the p125 subunit and E2F1-activated transcription. Mol. Cell. Biol. **19:**4935–4943.
46. **Shiyanov, P., A. Nag, and P. Raychaudhuri.** 1999. Cullin 4A associates with the UV-damaged DNA-binding protein DDB. J. Biol. Chem. **274:**35309–35312.
47. **Smith, M. L., J. M. Ford, M. C. Hollander, R. A. Bortnick, S. A. Amundson, Y. R. Seo, C. X. Deng, P. C. Hanawalt, and A. J. Fornace, Jr.** 2000. p53-mediated DNA repair responses to UV radiation: studies of mouse cells lacking p53, p21, and/or gadd45 genes. Mol. Cell. Biol. **20:**3705–3714.
48. **Tang, J., and G. Chu.** 2002. Xeroderma pigmentosum complementation group E and UV-damaged DNA-binding protein. DNA Repair **1:**601–616.
49. **Toledo, F., and G. M. Wahl.** 2006. Regulating the p53 pathways: in vitro hypotheses, in vivo veritas. Nat. Rev. Cancer **6:**909–923.
50. **Wahl, G. M., and A. M. Carr.** 2001. The evolution of diverse biological responses to DNA damage: insight from yeast and p53. Nat. Cell Biol. **3:**E277–E284.
51. **Wakasugi, M., A. Kawashima, H. Morioka, S. Linn, A. Sancar, T. Mori, O. Nikaido, and T. Matsunaga.** 2002. DDB accumulates at DNA damage sites immediately after UV irradiation and directly stimulates nucleotide excision repair. J. Biol. Chem. **277:**1637–1640.
52. **Wang, H., L. Zhai, J. Xu, H. Y. Joo, S. Jackson, H. Erdjument-Bromage, P. Tempst, Y. Xiong, and Y. Zhang.** 2006. Histone H3 and H4 Ubiquitylation by the CUL4-DDB-ROC1 Ubiquitin Ligase Facilitates Cellular Response to DNA Damage. Mol. Cell **22:**383–394.
53. **Xirodimas, D., M. K. Saville, C. Edling, D. P. Lane, and S. Lain.** 2001. Different effects of p14ARF on the levels of ubiquitinated p53 and Mdm2 in vivo. Oncogene **20:**4972–4983.
54. **Yoon, T., A. Chakrabortty, R. Franks, T. Valli, H. Kiyokawa, and P. Raychaudhuri.** 2005. Tumor-prone phenotype of the DDB2-deficient mice. Oncogene **24:**469–478.
55. **Zhang, Y.-W., D. M. Otterness, G. G. Chiang, W. Xie, Y.-C. Liu, F. Mercurio, and R. T. Abraham.** 2005. Genotoxic stress targets human Chk1 for degradation by the ubiquitin-proteasome pathway. Mol. Cell **19:**607–618.
56. **Zhou, B. B., and S. J. Elledge.** 2000. The DNA damage response: putting checkpoints in perspective. Nature **408:**433–439.
57. **Zotter, A., M. S. Luisjsterburg, D. O. Warmerdam, S. Ibrahim, A. Nigg, W. A. van Cappellen, J. H. J. Hoeijmakers, R. van Driel, W. Vermeulen, and A. B. Houtsmuller.** 2006. Recruitment of the nucleotide excision repair endonuclease XPG to site of UV-induced DNA damage depends on functional TFIIH. Mol. Cell. Biol. **26:**8868–8879.